New leads for DPP IV inhibition: structure-based pharmacophore mapping and virtual screening study

Ihab M. Almasri, Mutasem O. Taha & Mohammad K. Mohammad

Archives of Pharmacal Research

ISSN 0253-6269

Arch. Pharm. Res.
DOI 10.1007/s12272-013-0224-1

Springer

Arch. Pharm. Res.
DOI 10.1007/s12272-013-0224-1

Archives of Pharmacal Research
www.springer.com/12272

RESEARCH ARTICLE

New leads for DPP IV inhibition: structure-based pharmacophore mapping and virtual screening study

Ihab M. Almasri · Mutasem O. Taha · Mohammad K. Mohammad

Abstract Dipeptidyl peptidase IV (DPP IV) is an attractive target for the development of new antidiabetic drugs. DPP IV inhibitors improve glycemic control by preventing the rapid inactivation of the incretin hormones; glucagon-like peptide 1 (GLP-1) and glucose-dependent insulinotropic peptide. In the current study, virtual screening, using 2D and 3D filters implemented in a hierarchical cascade, was employed to identify new DPP IV inhibitors. Co-crystallized ligands, with potent DPP IV-inhibitory activities, were utilized to generate structure-based pharmacophore models using DS Visualizer software. The derived pharmacophore maps were validated using in-house built database containing active and inactive DPP IV inhibitors. Subsequently, the optimum validated pharmacophore model was used as a search query against two 3D-databases (NCI and in-house built drug databases). Further hit filtration was carried out employing 2D virtual filters based on Lipinski's rule of 5; number of rotatable bonds and other physicochemical filters. 3D filter using high-throughput molecular docking was also applied. As a result, 5 novel DPP IV inhibitors were discovered as potential lead compounds and later confirmed via in vitro bioassay.

Keywords DPP IV · Structure-based pharmacophore · High-throughput docking · Lead inhibitors · Virtual screening

I. M. Almasri (✉)
Department of Chemistry and Pharmaceutical Chemistry, Faculty of Pharmacy, Al-Azhar University, Gaza, Gaza Strip
e-mail: i.masri@alazhar-gaza.edu

M. O. Taha · M. K. Mohammad
Department of Pharmaceutical Sciences, Faculty of Pharmacy, University of Jordan, Amman, Jordan

Introduction

Type two diabetes mellitus, formerly known as Non-insulin dependent diabetes mellitus (NIDDM) is characterized by elevated blood glucose level that results from inadequate insulin action in insulin-sensitive tissues (Moller 2001). Various potential targets are being investigated for drug development to treat NIDDM and insulin resistance. Of these, Dipeptidyl peptidase IV (DPP IV) has emerged as a promising target with vast clinical potential. Indeed, the latter has triggered a wealth of studies to further characterize the enzyme and the therapeutic applications of its inhibitors (Engel et al. 2003). A compelling body of evidence confirmed a strong correlation between DPP IV and many diseases such as diabetes, obesity and tumor progression, making it an attractive target in drug discovery research (Cheng et al. 2002; Pospisilik et al. 2002). DPP IV is a serine protease responsible for in vivo degradation of endogenous peptides by cleaving the penultimate (N-terminal) proline or alanine. Several bioactive peptides are among its known targets, e.g., growth hormone releasing hormone and substance P (Frohman et al. 1989; Ahmad et al. 1992). However, its most clinically attractive substrates are incretins: glucagon-like peptide 1 (GLP-1) and glucose-dependent insulinotropic polypeptide (GIP). These are incretins released from the gut in response to carbohydrate intake and play an important role in maintaining glucose homeostasis (Drucker 2003; Efendic and Portwood 2004). Together, they are responsible for up to 70 % of insulin secreted following a meal (Nauck et al. 1986). Moreover, they promote β-cell regeneration and inhibit apoptosis of β-cells in the pancreas (Brubaker and Drucker 2004). However, the effects of incretins in type 2 diabetic patients are severely diminished and inhibition of DPP IV has been shown to improve glucose tolerance in these

Published online: 06 August 2013

patients by enhancing the insulinotropic effects of GLP-1 (Ahren et al. 2004; Nauck et al. 2004). As a result, the search for inhibitors of DPP IV for the treatment of type 2 diabetes is an active area of research (Weber 2004; Demuth et al. 2005).

Most DPP IV inhibitors were designed according to the substrate P1 site structure (occupied by proline), namely the proline-like compounds. In addition to the proline-like compounds, a variety of non-peptide-like and reversible DPP IV inhibitors were also discovered via high-throughput screening and offered new recognition motifs to DPP IV (Frohman et al. 1989). Three general classes of DPP IV inhibitors with in vivo efficacy can be described: (1) reversible substrate analogs; (2) covalently modifying substrate analogs; (3) reversible non-peptide heterocyclic compounds (Demuth et al. 2005). Both the reversible and covalently modifying substrate analog inhibitors take advantage of the high preference of DPP IV for proline binding within the S1 hydrophobic pocket. These inhibitors are generally amide derivatives of pyrrolidine (α-aminoacylpyrrolidines) or thiazolidine (a-aminoacylthiazolidines), which bind with even greater affinity. Examples include valine-pyrrolidide (**1**) (Neubert et al. 1991) and isoleucine-thiazolidide (**2**) (Schon et al. 1991) (Fig. 1). The covalently modifying inhibitors contain in addition an electrophilic group at the 2-position of the pyrrolidine or thiazolidine ring and are even more potent. The most common group is cyano, which is capable of forming an enzyme-imidate adduct with the active site Ser630 and is present in vildagliptin (**3**) (Villhauer et al. 2003) and saxagliptin (**4**) (Augeri et al. 2005) (Fig. 1).

The reversible non-peptide heterocyclic inhibitors include compound (**5**) (Brockunier et al. 2004) (Fig. 1), and other compounds from a diverse array of classes (e.g., compound **6**). These do not contain a pyrrolidine or thiazolidine ring to bind within the S1 pocket. Instead, compound **5** has a piperazine ring system and binds to the enzyme with the amide moiety in an orientation opposite to that of substrate analog inhibitors so that the 2,5-difluorophenyl group binds within the S1 hydrophobic pocket (Brockunier et al. 2004). Other classes of known inhibitors include; xanthine, aminomethylpyrimidine and isoquinoline compounds (Demuth et al. 2005). Several new DPP IV inhibitors are currently in clinical trials (Hunziker et al. 2005). The first DPP IV inhibitor Januvia (sitagliptin, **8**), manufactured by Merck & Co., was approved by the FDA as the first of a new class of pharmacologic agents for the treatment of type 2 diabetes. Clinical data show that Januvia offers many potential advantages, including low risk of hypoglycemia, weight neutral or modest weight loss, synergistic effects to metformin and convenient daily dosing. (Miller and St. Onge 2006). A number of adverse effects, however, were also observed with the drug, including increased risk for upper respiratory tract infection, sore throat, and diarrhea (Barnett 2006). Indeed, patient compliance would be significantly improved via the introduction of new drugs in the same pharmacologic class that have fewer adverse effects. Hence, the development of

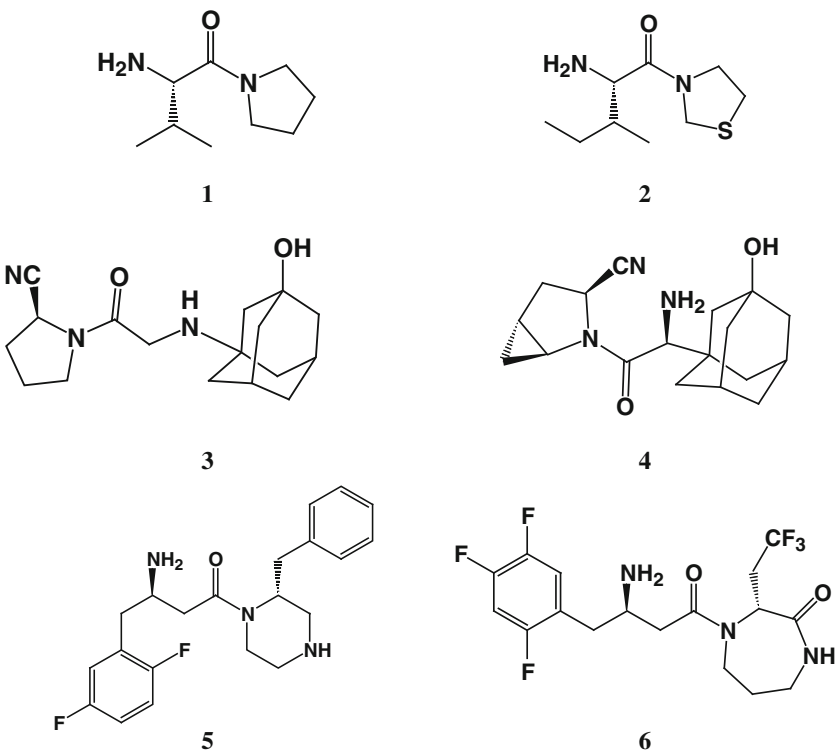

Fig. 1 Structures of different classes of DPP IV inhibitors

a faster and more accurate system to discover and optimize the structure activity relationship (SAR) of new DPP IV inhibitors with better therapeutic efficacies and safety profiles is highly desirable.

According to a plethora of published literature, the hit rate of DPP IV inhibitors by high throughput screening (HTS) is very low (Ward et al. 2005), yielding only about 0.012 % for actives with 30 % inhibition at 10 μM. This low hit rate lead to the emergence of virtual screening (VS) as an alternative method to discover novel DPP IV inhibitors. Ward et al. (2005), developed a virtual screening protocol combining pharmacophore filtering with compound docking to discover DPP IV inhibitors of low molecular weight. Their strongest compound inhibited 81.9 % of the DPP IV activity at 30 mM. Furthermore, Rummey et al. (2006), presented a pharmacophore constrained docking method by screening a small primary aliphatic amines fragment database to identify fragments that could be placed in S1 and S2 sites of DPP IV. The best binders in their study showed promising results with IC_{50} of 2.3 mM for DPP IV. Recently, we have developed a robust, ligand-based three-dimensional (3D) pharmacophores that were used as database search queries to mine 3D compound libraries for new DPP IV inhibitors. The models captured several potential hits and one of our interesting potent anti-DPP IV hits was the fluoroquinolone gemifloxacin ($IC_{50} = 1.12$ μM) (Al-masri et al. 2008). In this article, a 3D structure-based pharmacophore modeling, based on X-ray crystallographic image of ligand-DPP IV complexes, followed by virtual screening is reported. The criteria adopted for the validation of developed pharmacophoric queries were based on submitting the pharmacophoric queries to an in-house database of reported DPP IV inhibitors. The optimum pharmacophoric model was then used as a filter in hierarchical filtration scheme to screen the virtual hits to identify new DPP IV inhibitors.

Materials and methods

Software and hardware

The following software packages were utilized in the present research.

- Discovery Studio (DS) Visualizer 2.0, Accelrys Inc. (www.accelrys.com), USA.
- CATALYST (Version 4.11), Accelrys Inc. (www.accelrys.com), USA.
- OMEGA (Version 2.3.2), OpenEye Scientific Software (www.eyesopen.com), USA.
- FRED (Version 2.1.5), OpenEye Scientific Software, (www.eyesopen.com), USA.
- Filter (Version 2.0.1), OpenEye Scientific Software, (www.eyesopen.com), USA.

Structure-based pharmacophore modeling was performed using DS visualizer and the in silico hits virtual screening was performed using CATALYST software installed on a Silicon Graphics Octane2 desktop workstation equipped with a dual 600 MHz MIPS R14000 processor (1.0 GB RAM) running the Irix 6.5 operating system. Hits filtration and docking were performed using FILTER, FRED and OMEGA software installed on Pentium 4 PC.

Pharmacophore model generation and validation

For the manual generation of structure-based pharmacophore models for DPP IV inhibitors, the software DS Visualizer 2.0 was applied. The ligand–protein interactions of four diverse DPP IV ligand–protein complexes found in the protein data bank (PDB) were investigated (see Figs. 2, 3) (PDB codes: 1RWQ with aminomethylpyrimidines (**7**) (Peters et al. 2004); 1X70 with triazolopiperazines (**8**) (Kim et al. 2005); 2FJP with triazolopyridine (**9**) (Edmondson et al. 2006); 2HHA with oxadiazole inhibitor (**10**) (Xu et al. 2006), resolution between 2.1-2.4 Å). A pharmacophore model for each PDB entry was derived from the protein–ligand interaction pocket by identifying complementary interactions. Figure 3 shows the identified pharmacophore features of the inhibitors derived from crystal structures of the four DPP IV-inhibitor complexes. 3D pharmacophores were constructed from a defined set of five types of chemical features: hydrogen bond donors and acceptors; positively ionized; hydrophobic aromatic and hydrophobic interactions. To select optimum pharmacophoric model, the validity of the developed pharmacophore maps was carried out using database search. A 3D database (DPP IV-3DDB) was built using reported active and inactive molecules from all the categories of DPP IV inhibitors. The database contained 358 compounds (341 active DPP IV inhibitors and 17 inactive molecules). An acceptable optimum pharmacophoric query should be able to pick up high number of the active DPP IV inhibitors and should exclude the inactive molecules from the built database.

In-silico screening for new DPP IV inhibitors

A schematic diagram showing the virtual screening strategy adopted in this work is shown in Fig. 4. The best pharmacophore model for DPP IV inhibitors with the highest recovery and selectivity (HYPO-2HHA, Fig. 3) was used as 3D-search query against two multi-conformer structural databases, namely, the national cancer institute

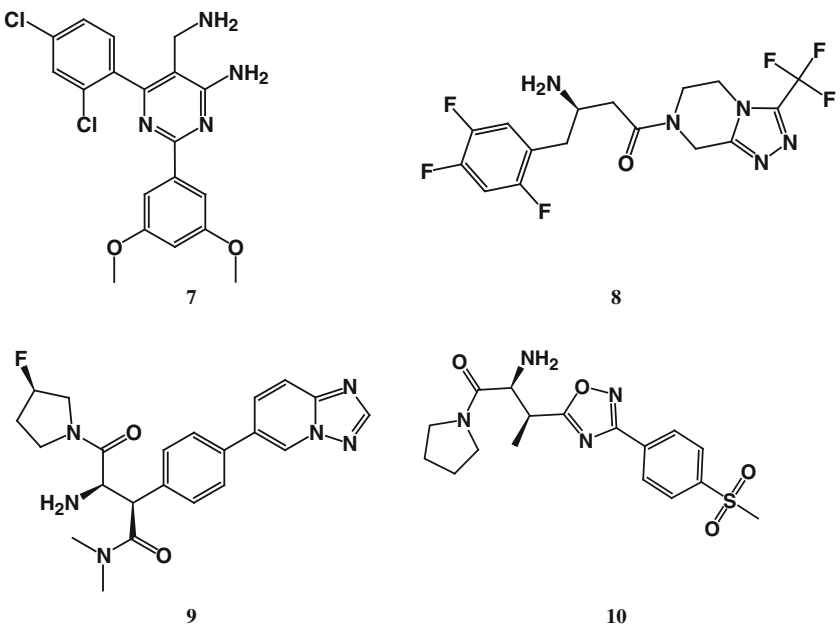

Fig. 2 Structures of the four co-crystallized DPP IV inhibitors (**7**; PDB 1RWQ, **8**; PDB 1X70, **9**; PDB 2FJP and **10**; PDB 2HHA)

list of compounds (NCI database, includes 238,819 compounds) (Catalyst 2005) and our in-house built multi-conformer database of established drug molecules (includes 1,490 compounds) via the "Best Flexible Search" option within CATALYST. The captured hits were filtered according to their physicochemical properties utilizing the program FILTER (FILTER 2005). The following filter criteria were applied to remove undesirable non-drug like compounds: (i) the maximum limit of the molecular weight was set to 500 Da, (ii) the maximum for the AlogP value was set to 5, (iii) the number of heavy atoms was limited to 15–30, (iv) at least 2 and at maximum 15 atoms of the compound had to be a heteroatom, (v) the maximum number of hydrogen bond acceptor (HBA) atoms was allowed to be 10, whereas the maximum number of hydrogen bond donors was restricted to 5. The number of rotatable bonds was restricted to a maximum of 10. Moreover, the FILTER software eliminates about 100 unstable/toxic/reactive functional groups. The remaining compounds were exported as MDL SD-file and subjected to the molecular docking screening approach.

High throughput docking

The conformational space of the filtered compounds (603 molecules) was explored employing OMEGA software (OMEGA 2008). In our computations, we generated a maximum of 100 conformations per molecule and used an ewindow (defines the strain energy range) of 25.0 kcal/mol and an RMSD cutoff of 1.0 Å. FRED was used subsequently to dock the multi-conformer filtered compounds. FRED strategy is to exhaustively dock/score all possible positions of each ligand in the binding site. The exhaustive search is based on rigid rotations and translations of each conformer within the binding site defined by a box created by the users (FRED 2009). The filtered compounds were docked into the binding site of DPP IV (PDB code: 2G63, resolution = 2.0 Å). The ligand molecule was removed from the binding site and hydrogen atoms were added to protein structure using the program DS Visualizer. Default parameters were employed in the docking experiment with the following modifications were performed: *Addbox* parameter was set to 2.00 and *Clash_checking* parameter was set to 0.5. The docked poses were scored using the Chemgauss2 scoring function.

In vitro DPP IV enzyme inhibition assay

Each hit compound was dissolved in DMSO and then it was suitably diluted with Tris buffer (pH 7.5) for subsequent enzymatic assay. The assay was conducted using DPP IV Drug Discovery Kit (Biomol, Germany), which is based on the cleavage of chromogenic substrate (H-Gly-Pro-*para*-Nitroaniline) by DPP IV to release *para*-nitroaniline (pNA) measured at 405 nm. For further procedure details see Al-masri et al. (2008).

Results and discussion

Virtual screening using pharmacophore model

At the beginning of our virtual screening workflow, pharmacophore modeling, a fast and well proven virtual screening technique, was applied. The software DS Visualizer was used to derive manual structure-based pharmacophore models

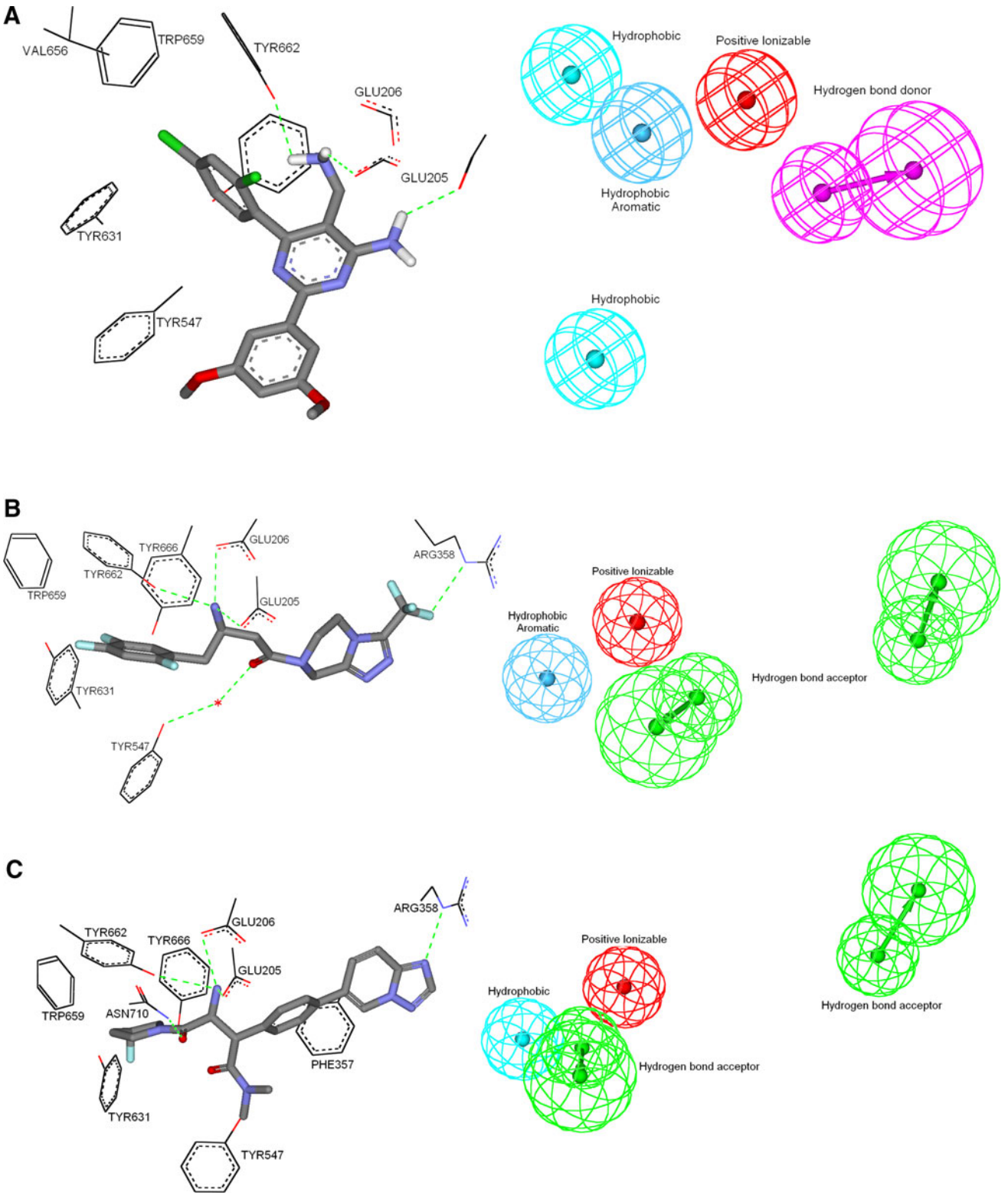

Fig. 3 Putative ligand–protein interactions of the four co-crystallized DPP IV inhibitors, **7** (**a**), **8** (**b**), **9** (**c**), and **10** (**d**), along with their corresponding structure-based pharmacophoric maps. **a** PDB 1RWQ with HYPO-1RWQ, **b** PDB 1X70 with HYPO-1X70, **c** PDB 2FJP with HYPO-2FJP and **d** PDB 2HHA with HYPO-2HHA. *Green lines* represent the hydrogen bonds, (Catalytic site residues are represented as *lines* while the co-crystallized ligands are displayed in *sticks*)

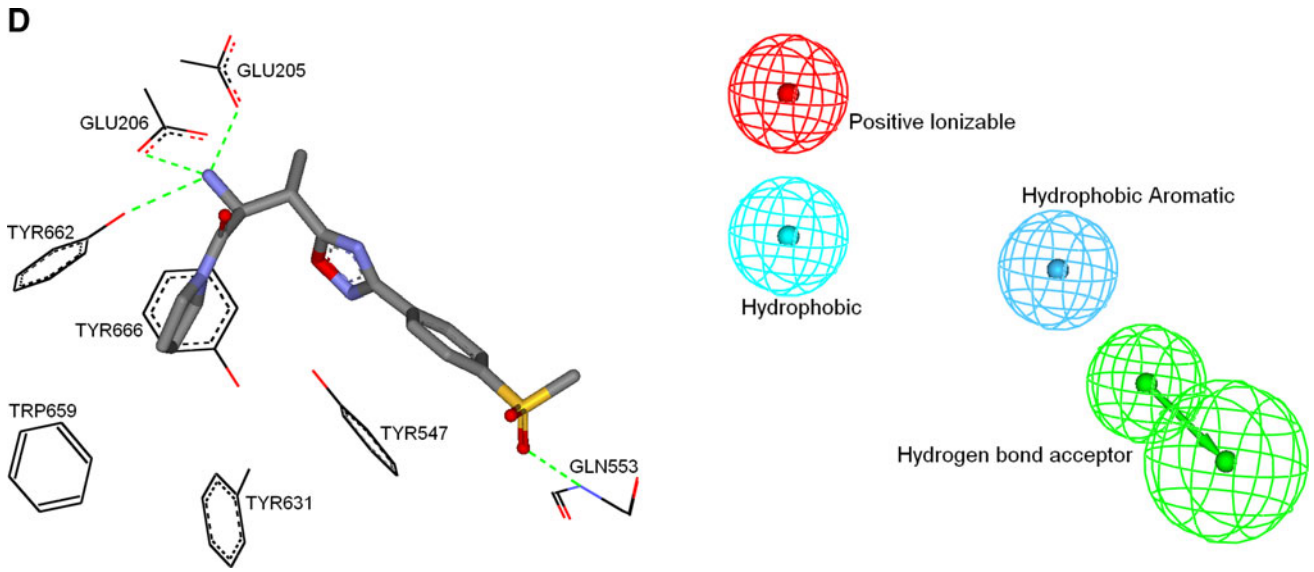

Fig. 3 continued

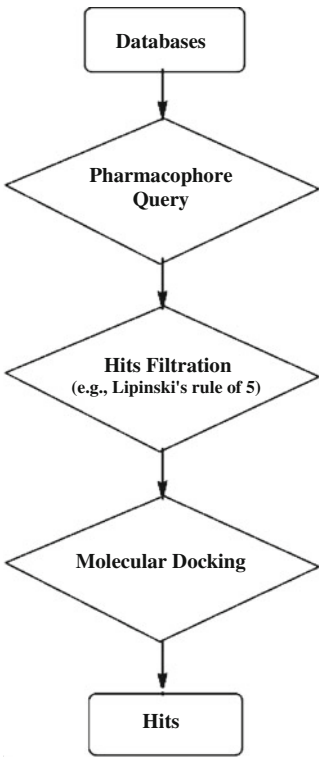

Fig. 4 Schematic representation of the steps adopted in the virtual screening

from crystallographic data of DPP IV-inhibitor complexes found in the Brookhaven PDB. The selected crystallographic complexes were of high resolution (2.1–2.4 Å) and for potent reversible non-peptide heterocyclic inhibitors (don't containing nitrile group). The selected features for the generated models were based on important complementary interactions between the DPP IV target and the corresponding inhibitors. For example, the crystallographic image of aminomethylpyrimidine (**7**, Fig. 2) derivative inhibitor within DPP IV binding pocket (PDB code; 1RWQ, Fig. 3) shows that the aliphatic amino group fits perfectly in the N-terminal recognition region Glu205-Glu206-Tyr662, forming strong hydrogen-bond-reinforced ionic interaction (corresponds to the positively ionized feature in HYPO-1RWQ, Fig. 3a). The dichlorophenyl ring lies within the hydrophobic S1 pocket Tyr631-Val656-Trp659-Tyr662-Tyr666-Val711 forming aromatic π–π and hydrophobic interactions (corresponds to the hydrophobic and hydrophobic aromatic features in the generated model). Furthermore, the aromatic amine is within the hydrogen-bond interaction range with carbonyl oxygen of Glu205 (corresponds to the hydrogen bond donor feature). Finally, the methoxy group can form a hydrophobic interaction with Tyr547 (corresponds to the second hydrophobic feature). An additional three structure-based pharmacophores, HYPO-1X70, HYPO-2FJP and HYPO-2HHA were generated in a similar manner (Fig. 3 b–d respectively).

The discriminatory power of the resulting pharmacophore models was estimated by screening a database comprising 358 DPP IV inhibitors (see "Materials and methods" section). The validation results (Table 1) were expressed as the percentage of retrieved active and inactive hits. The query HYPO-2HHA (Fig. 3d) picked 217 DPP IV inhibitors out of 341 and just 5 inactive molecules out of 17 present in the built database. HYPO-2HHA has the characteristic features required for an ideal pharmacophoric query, because it possesses the important interactions required for DPP IV inhibitors, and performs satisfactorily

Table 1 Evaluation of the generated structure-base pharmacophores using the in-house DPP IV database (DPP IV-3DDB)

Pharmacophore model	PDB code	Ref.	Resolution	Total Hits[a]	Active hits	Inactive hits
HYPO-2HHA	2HHA	Pospisilik et al. (2002)	2.3	222	217 (0.64)	5 (0.29)
HYPO-1RWQ	1RWQ	Pei et al. (2006)	2.2	14	14 (0.04)	0 (0)
HYPO-1X70	1X70	Pei et al. (2007)	2.1	113	103 (0.30)	10 (0.59)
HYPO-2FJP	2FJP	Peters et al. (2004)	2.4	197	190 (0.56)	7 (0.41)

[a] Total hits picked by the model from the in-house database, values in parentheses are the hit rates for each category

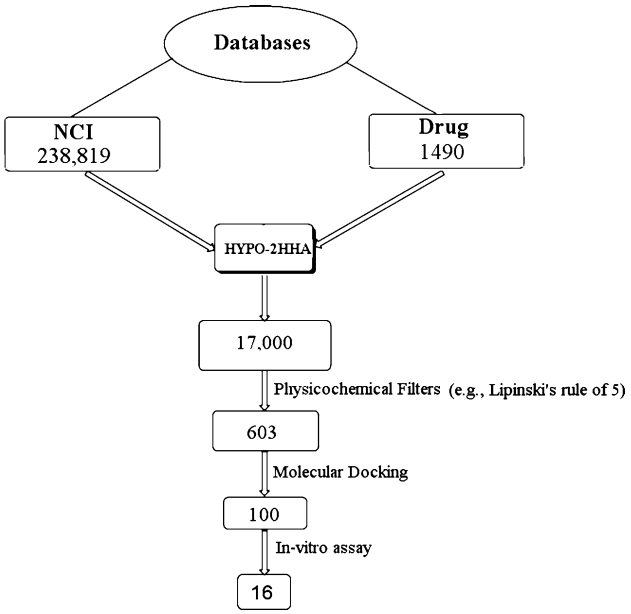

Fig. 5 The results obtained from the virtual screening of the two databases (NCI, drug). The *numbers* given in the figure represent the number of molecules after employing the filters

as screening query in the pharmacophore validation step. Hence, HYPO-2HHA was selected for virtual screening purpose.

Virtual screening with the help of HYPO-2HHA against two libraries of compounds comprising a total of 240,309 structures resulted in the selection of 17,000 hits from the NCI and in-house built drug databases. Further refinement of these hits was carried out by the FILTER software which reduced the number of hits to 603 (Fig. 5). FILTER attempts to remove all compounds containing functional groups known to be reactive or resembling toxic entities and those with unsatisfactory physicochemical properties. These simple filters serve to reduce the incidence of false positives, improve the downstream properties of the compounds (pharmacokinetics, metabolism, etc.), and provide druggable leads from the outset. FILTER's criteria for passing or failing a given molecule fall into three categories: physical properties, atomic and functional-group content, and molecular graph topology. After that, the 603 filtered hits obtained from virtual screening were docked into the binding site of DPP IV using FRED software. FRED was reported to illustrate good overall performance, particularly in virtual high-throughput screening experiments (Vigers and Rizzi 2004). The docking filtration step resulted in 50 hits having high FRED Chemgauss2 score (FRED 2009). The potential lead compounds that showed DPP IV inhibition activity were listed in Table 2 and Fig. 6. The first 11 hits (compounds **11**–**21**, Table 2; Fig. 6) were previously reported as DPP IV inhibitors in a ligand-based pharmacophore screening approach and the most potent hit was gemifloxacin (IC_{50} = 1.1 μM) (Al-masri et al. 2008). Moreover, gemifloxacin was found to lower significantly plasma glucose concentrations after oral glucose challenge (i.e., OGTT) in Balb/c mice (Al-masri et al. 2008). The remaining 5 hits (compounds **22**–**26**,

Table 2 The hit molecules captured by HYPO-2HHA and their corresponding FRED docking scores and their in vitro bioactivities

Tested hits[a]	NCI codes/ names	In vitro anti-DPP IV activity	
		Percentage inhibition at 10 μM[b]	IC_{50} (μM)
11	337722	52.5	–
12	661075	20.0	–
13	661077	25.0	–
14	382748	23.5	–
15	382931	26.0	–
16	138927	18.0	–
17	339919	33.0	–
18	661081	15.0	–
19	134131	18.0	–
20	67053	20.0	–
21	Gemifloxacin	65.0	1.12[b]
22	Paroxetine	20.0	–
23	47527	20.0	–
24	211844	37.0	–
25	211295	40.0	–
26	163391	17.0	–

[a] Structures as in Fig. 6

[b] The percentage inhibition values for compounds **11**–**21** were reported in reference (Al-masri et al. 2008)

Fig. 6 The chemical structures of the active hits (their experimental bioactivities as in table 2)

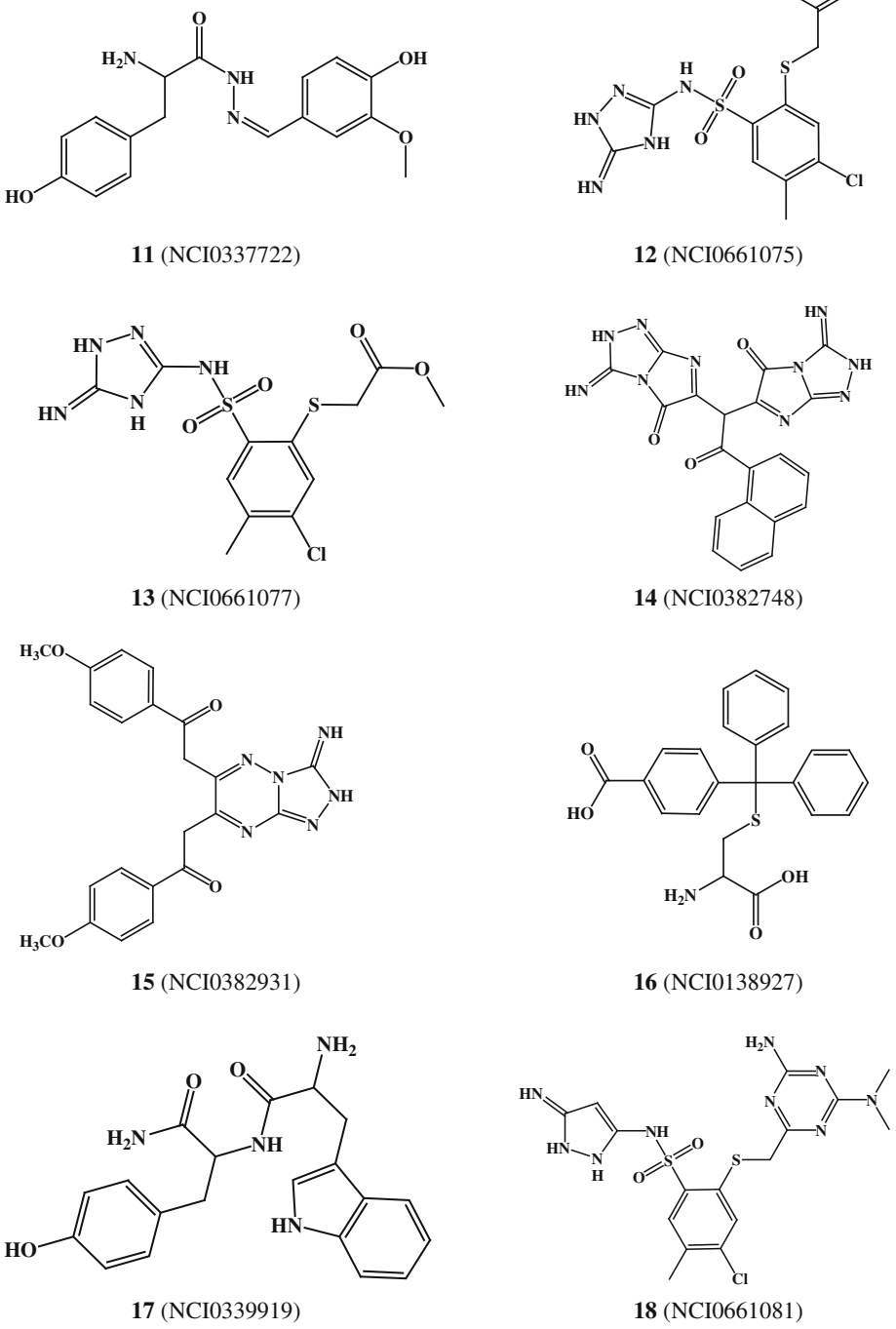

11 (NCI0337722)

12 (NCI0661075)

13 (NCI0661077)

14 (NCI0382748)

15 (NCI0382931)

16 (NCI0138927)

17 (NCI0339919)

18 (NCI0661081)

Table 2; Fig. 6) are new hits that can be used as potential leads for further optimization.

Paroxetine (**22**, Fig. 6), a piperidine derivative, is another hit captured by HYPO-2HHA and was found to have DPP IV inhibitory activity (20 % at 10 μM). Interestingly, a group of piperidine derivatives were discovered recently as potent and selective DPP IV inhibitors (Pei et al. 2007), which could consolidate our finding regarding paroxetine DPP IV inhibition activity

Comparison of HYPO-2HHA with the binding site of DPP IV

The pharmacophore features obtained by structured-based pharmacophore modeling can be compared with the structure of DPP IV binding site to identify probable residues important for inhibition. The features in HYPO-2HHA, as well as, the alignment of **11** (NCI0337722) (inhibitory percentage at 10 μM = 52.5 %), as proposed

Fig. 6 continued

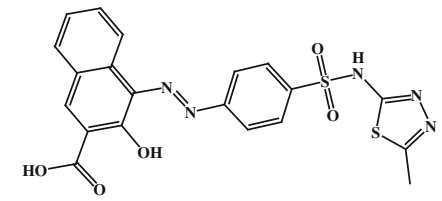

19 (NCI0134131)

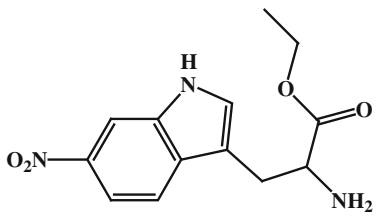

20 (NCI0067053)

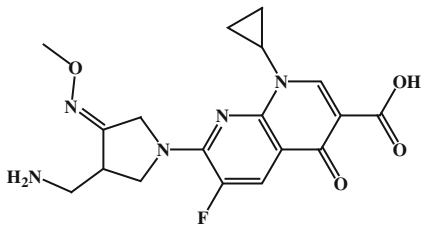

21 (Gemifloxacin)

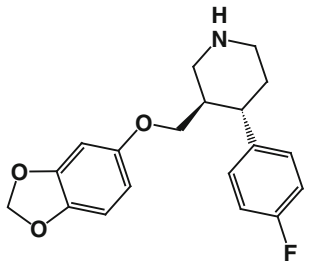

22 (Paroxetine)

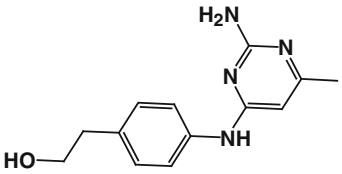

23 (NCI0047527)

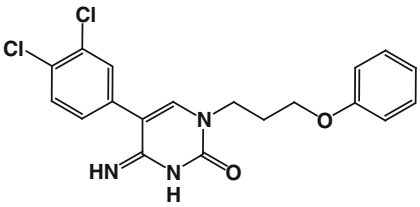

24 (NCI0211844)

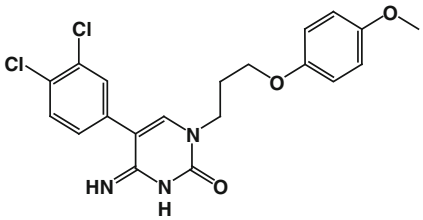

25 (NCI0211295)

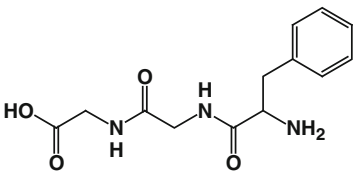

26 (NCI0163391)

by this pharmacophore, were compared with the corresponding structure as it docks into the binding pocket of DPP IV (PDB code: 2G63, resolution 2.0 Å), (Pei et al. 2006) as in Fig. 7. The docking experiment was performed employing FRED docking engine and Chemgauss2 scoring function. A marked similarity was observed between the features proposed by the pharmacophore models and the ligand binding features in the docked structures.

In the highest-ranking docked pose of **11** (Fig. 7a) the carboxylic acid moiety of Glu205 binds to the amino group of **11** via a hydrogen-bond-reinforced ionic interaction corresponding to amino group mapping with a positive ionizable feature in HYPO-2HHA (Fig. 7b). Moreover, the oxygen of the phenolic hydroxyl group of **11** seems to be hydrogen-bonded to the NH of Trp629, which agrees with mapping the same hydroxyl by HBA feature in HYPO-2HHA, as in Fig. 7a. Similarly, the close proximity of methoxy-substituted phenyl ring in **11** with the aromatic indole ring of Trp629 correlates nicely with the hydrophobic aromatic feature in HYPO-2HHA. Finally, the docking experiment has placed the second phenolic ring in the hydrophobic S1 pocket which comprises Tyr631-Val656-Trp659-Tyr662-Tyr666. This corresponds perfectly with the phenolic ring mapping to the hydrophobic feature in HYPO-2HHA (Fig. 7).

On the other hand, the validity of HYPO-2HHA can be further established by comparing the way it maps **22** (paroxetine) with the docked pose of this hit inside the binding pocket of DPP IV. As shown in Fig. 7 c, d, the HBA feature mapping the oxygen in the 1,3-dioxolane in **22** (Fig. 7d) corresponds to hydrogen-bonding with Tyr631 in the docked pose (Fig. 7c). The close proximity of

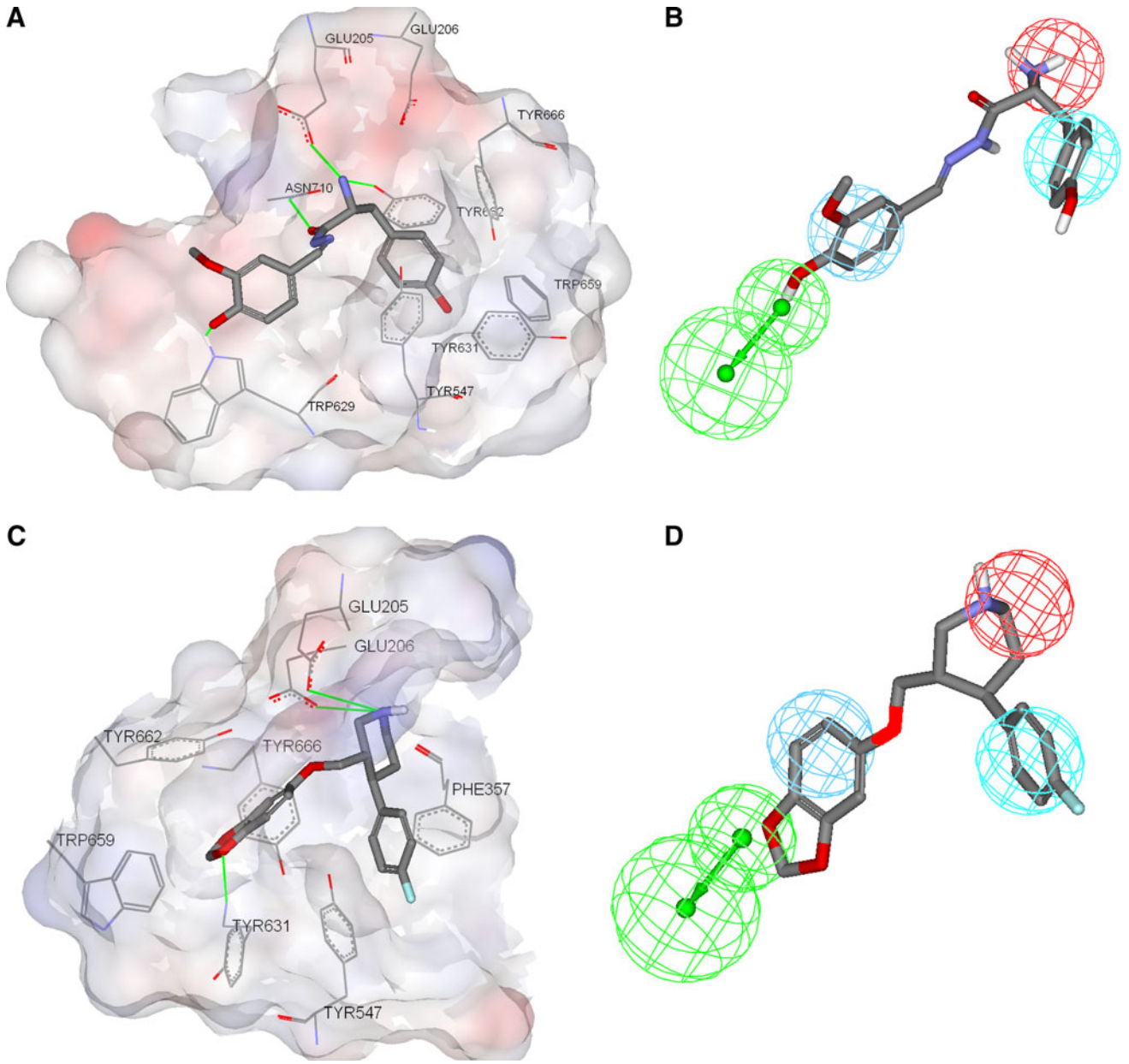

Fig. 7 Two DPP IV hits (**11** and **22**, Fig. 6; Table 2) docked in the binding pocket of DPP IV (PDB code: 2G63, resolution 2.00 Å) by FRED docking engine. **a** An optimal docked pose of **11** (inhibitory percentage at 10 μM = 52.5 %); **b** HYPO-2HHA fitted against **11**. **c** An optimal docked pose of **22** (Paroxetine, inhibitory percentage at 10 μM = 20 %) into the binding pocket of DPP IV, **d** HYPO-2HHA fitted against **22**. The protein solvent-accessible surface is colored by electrostatic potential, *green lines* represent the potential hydrogen bonds, catalytic site residues are represented as *lines* while the docked hits are displayed in *sticks*

piperidine nitrogen of **22** to the carboxyl groups of Glu205 and Glu206 in the docked structure (Fig. 7c) suggests their mutual hydrogen-bond-reinforced ionic interaction. This proposition is supported by a positive ionizable feature mapping the same nitrogen in HYPO-2HHA (Fig. 7). Similarly, the fluorophenyl of **22** is mapped by a hydrophobic (Hbic) feature in HYPO-2HHA (Fig. 7d) corresponding to hydrophobic interaction with the phenyl ring of Phe357 in the docked pose (Fig. 7c). Finally, the benzodioxol ring of **22** is docked within the π-rich ring system of the hydrophobic S1 pocket, which comprises Tyr631-Trp659-Tyr662-Tyr666, suggesting the existence of significant mutual van der Waals' stacking interactions, which correlate with a hydrophobic aromatic feature mapping the benzodioxol ring in HYPO-2HHA (Fig. 7D). The binding orientations of compounds **11** and **22** substantiated the features mapped by the pharmacophore model. It is suggested that correct mapping to four features

is sufficient to successfully identify specific DPP IV inhibitors. Therefore, the pharmacophore model is expected to help in the identification of new classes of DPP IV inhibitors using virtual screening.

Acknowledgments The authors wish to thank the Deanship of Scientific Research and Hamdi-Mango Center for Scientific Research at the University of Jordan for their generous funds. The authors would like to thank also the Open-Eye Scientific Software for providing us a free license of FRED, OMEGA and FILTER software.

References

Ahmad, S., L. Wang, and P.E. Ward. 1992. Dipeptidyl(amino)peptidase IV and aminopeptidase M metabolize circulating substance P in vivo. *Journal of Pharmacology and Experimental Therapeutics* 260: 1257–1261.

Ahren, B., M. Landin-Olsson, P. Jansson, M. Svensson, D. Holmes, and A. Schweizer. 2004. Inhibition of dipeptidyl peptidase-4 reduces glycemia, sustains insulin levels, and reduces glucagon levels in type 2 diabetes. *Journal of Clinical Endocrinology and Metabolism* 89: 2078–2084.

Al-masri, I., M. Mohammad, and M. Taha. 2008. Discovery of New DPP IV Inhibitors via pharmacophore Modeling and QSAR Analysis followed by in silico screening. *ChemMedChem* 3: 1763–1779.

Augeri, D.J., J.A. Robl, D.A. Betebenner, D.R. Magnin, A. Khanna, J.G. Robertson, A. Wang, L.M. Simpkins, P. Taunk, Q. Huang, S.-P. Han, B. Abboa-Offei, M. Cap, L. Xin, L. Tao, E. Tozzo, G.E. Welzel, D.M. Egan, J. Marcinkeviciene, S.Y. Chang, S.A. Biller, M.S. Kirby, R.A. Parker, and L.G. Hamann. 2005. Discovery and preclinical profile of saxagliptin (BMS-477118): A highly potent, long-acting, orally active dipeptidyl peptidase IV inhibitor for the treatment of type 2 diabetes. *Journal of Medicinal Chemistry* 48: 5025–5037.

Barnett, A. 2006. DPP-4 inhibitors and their potential role in the management of type 2 diabetes. *International Journal of Clinical Practice* 60: 1454–1470.

Brockunier, L.L., J. He, L.F. Colwell Jr, B. Habulihaz, H. He, B. Leiting, K.A. Lyons, F. Marsilio, R.A. Patel, Y. Teffera, J.K. Wu, N.A. Thornberry, A.E. Weber, and E.R. Parmee. 2004. Substituted piperazines as novel dipeptidyl peptidase IV inhibitors. *Bioorganic & Medicinal Chemistry Letters* 14: 4763–4766.

Brubaker, P.L., and D.J. Drucker. 2004. Minireview: Glucagon-like peptides regulate cell proliferation and apoptosis in the pancreas, gut, and central nervous system. *Endocrinology* 145(6): 2653–2659.

Catalyst User Guide, Accelrys Software Inc., San Diego, 2005.

Cheng, J.D., R.L. Dunbrack Jr, M. Valianou, A. Rogatko, R.K. Alpaugh, and L.M. Weiner. 2002. Promotion of tumor growth by murine fibroblast activation protein, a serine protease, in an animal model. *Cancer Research* 62: 4767–4772.

Demuth, H., C.H.S. McIntosh, and R.A. Pederson. 2005. Type 2 diabetes-therapy with dipeptidyl peptidase IV inhibitors. *Biochimica et Biophysica Acta* 1751: 33–44.

Drucker, D.J. 2003. Enhancing incretin action for the treatment of type 2 diabetes. *Diabetes Care* 26: 2929–2940.

Edmondson, S.D., A. Mastracchio, R.J. Mathvink, J. He, B. Harper, Y.J. Park, M. Beconi, J. Di Salvo, G.J. Eiermann, H. He, B. Leiting, J.F. Leone, D.A. Levorse, K. Lyons, R.A. Patel, S.B. Patel, A. Petrov, G. Scapin, J. Shang, R.S. Roy, A. Smith, J.K. Wu, S. Xu, B. Zhu, N.A. Thornberry, and A.E. Weber. 2006. (2S,3S)-3-Amino-4-(3,3-difluoropyrrolidin-1-yl)-*N*,*N*-dimethyl-4-oxo-2-(4-[1,2,4]triazolo[1,5-a]-pyridin-6-ylphenyl)butanamide: A selective alpha-amino amide dipeptidyl peptidase IV inhibitor for the treatment of type 2 diabetes. *Journal of Medicinal Chemistry* 49: 3614–3627.

Efendic, S., and N. Portwood. 2004. Overview of incretin hormones. *Hormone and Metabolic Research* 36(11–12): 742–746.

Engel, M., T. Hoffmann, L. Wagner, M. Wermann, U. Heiser, R. Kiefersauer, R. Huber, W. Bode, H.-U. Demuth, and H. Brandstetter. 2003. The crystal structure of dipeptidyl peptidase IV (CD26) reveals its functional regulation and enzymatic mechanism. *Proceedings of the National Academy of Sciences of the United States of America* 100: 5063–5068.

Filter, 2005. version 2.0 Users' Manual, OpenEye Scientific Software Inc., Santa Fe, New Mexico.

Fred, 2009. version 2.1.2 Users' Manual, OpenEye Scientific Software Inc., Santa Fe, New Mexico.

Frohman, L.A., T.R. Downs, E.P. Heimer, and A.M. Felix. 1989. Dipeptidylpeptidase IV and trypsin-like enzymic degradation of human growth hormone-releasing hormone in plasma. *Journal of Clinical Investigation* 83: 1533–1540.

Hunziker, D., M. Hennig, and J.U. Peters. 2005. Inhibitors of dipeptidyl peptidase IV-recent advances and structural views. *Current Topics in Medicinal Chemistry* 5: 1623–1637.

Kim, D., L. Wang, M. Beconi, G.J. Eiermann, M.H. Fisher, H. He, G.J. Hickey, J.E. Kowalchick, B. Leiting, K. Lyons, F. Marsilio, M.E. McCann, R.A. Patel, A. Petrov, G. Scapin, S.B. Patel, R.S. Roy, J.K. Wu, M.J. Wyvratt, B. Zhang, L. Zhu, N.A. Thornberry, and A.E. Weber. 2005. (2R)-4-oxo-4-[3-(trifluoromethyl)-5,6-dihydro[1,2,4]triazolo[4,3-a]pyrazin-7(8H)-yl]-1-(2,4,5-trifluorophenyl)butan-2-amine: A potent, orally active dipeptidyl peptidase IV inhibitor for the treatment of type 2 diabetes. *Journal of Medicinal Chemistry* 48: 141–151.

Miller, S.A., St. Onge, E.L. 2006. Sitagliptin: A dipeptidyl peptidase IV inhibitor for the treatment of type 2 diabetes. *Annals of Pharmacotherapy* 40: 1336–1343.

Moller, D.E. 2001. New drug targets for type II diabetes and the metabolic syndrome. *Nature* 414: 821–827.

Nauck, M.A., B. Baller, and J.J. Meier. 2004. Gastric inhibitory polypeptide and glucagon-like peptide-1 in the pathogenesis of type 2 diabetes. *Diabetes* 53: S190–S196.

Nauck, M.A., E. Homberger, E.G. Siegel, R.C. Allen, R.P. Eaton, R. Ebert, and W. Creutzfeldt. 1986. Incretin effects of increasing glucose loads in man calculated from venous insulin and C-peptide responses. *Journal of Clinical Endocrinology and Metabolism* 63: 492–498.

Neubert, K., Born, I., Faust, J., Heins, J., Barth, A., Demuth, H.U., Rahfeld, J.U., Steinmetzer, T., Preparation of amino acid amides as dipeptidyl peptidase IV inhibitors, German Patent Application. Number DD 296 075 A5, (1991).

Omega, 2008. version 2.1.0 Users' Manual, OpenEye Scientific Software Inc., Santa Fe, New Mexico.

Pei, Z., X. Li, K. Longenecker, T.W. Von Geldern, P.E. Wiedeman, T.H. Lubben, B.A. Zinker, K. Stewart, S.J. Ballaron, M.A. Stashko, A.K. Mika, D.W. Beno, M. Long, H. Wells, A.J. Kempf-Grote, D.J. Madar, T.S. McDermott, L. Bhagavatula, M.G. Fickes, D. Pireh, L.R. Solomon, M.R. Lake, R. Edalji, E.H. Fry, H.L. Sham, and J.M. Trevillyan. 2006. Discovery, structure-activity relationship, and pharmacological evaluation of (5-substituted-pyrrolidinyl-2-carbonyl)-2-cyanopyrrolidines as potent dipeptidyl peptidase IV inhibitors. *Journal of Medicinal Chemistry* 49: 3520–3535.

Pei, Z., X. Li, T.W. von Geldern, K. Longenecker, D. Pireh, K.D. Stewart, B.J. Backes, C. Lai, T.H. Lubben, S.J. Ballaron, D.W. Beno, A.J. Kempf-Grote, H.L. Sham, and J.M. Trevillyan. 2007. Discovery and structure–activity relationships of piperidinone- and piperidine-constrained phenethylamines as novel, potent,

and selective dipeptidyl peptidase IV inhibitors. *Journal of Medicinal Chemistry* 50: 1983–1987.

Peters, J.U., S. Weber, S. Kritter, P. Weiss, A. Wallier, M. Boehringer, M. Hennig, B. Kuhn, and B.M. Loeffler. 2004. Aminomethylpyrimidines as novel DPP-IV inhibitors: A 105-fold activity increase by optimization of aromatic substituents. *Bioorganic & Medicinal Chemistry Letters* 14: 1491–1493.

Pospisilik, J.A., S.G. Stafford, H.-U. Demuth, R. Brownsey, W. Parkhouse, D.T. Finegood, C.H.S. McIntosh, and R.A. Pederson. 2002. Long-term treatment with the dipeptidyl peptidase IV inhibitor P32/98 causes sustained improvements in glucose tolerance, insulin sensitivity, hyperinsulinemia, and β-cell glucose responsiveness in VDF (fa/fa) Zucker rats. *Diabetes* 51: 943–950.

Rummey, C., S. Nordhoff, M. Thiemann, and G. Metz. 2006. In silico fragment-based discovery of DPP-IV S1 pocket binders. *Bioorganic & Medicinal Chemistry Letters* 16: 1405–1409.

Schon, E., I. Born, H.U. Demuth, J. Faust, K. Neubert, T. Steinmetzer, A. Barth, and S. Ansorge. 1991. Dipeptidyl peptidase IV in the immune system. Effects of specific enzyme inhibitors on activity of dipeptidyl peptidase IV and proliferation of human lymphocytes. *Biological Chemistry Hoppe-Seyler* 372: 305–311.

Vigers, G.P., and J.P. Rizzi. 2004. Multiple active site corrections for docking and virtual screening. *Journal of Medicinal Chemistry* 47: 80–89.

Villhauer, E.B., J.A. Brinkman, G.B. Naderi, B.F. Burkey, B.E. Dunning, P. Kapa, B.L. Mangold, M.E. Russell, and T.E. Hughes. 2003. 1-[[(3-Hydroxy-1-adamantyl)amino] acetyl]-2-cyano-(S)-pyrrolidine: A potent, selective, and orally bioavailable dipeptidyl peptidase IV inhibitor with antihyperglycemic properties. *Journal of Medicinal Chemistry* 46: 2774–2789.

Ward, R.A., T.D. Perkins, and J. Stafford. 2005. Structure-based virtual screening for low molecular weight chemical starting points for dipeptidyl peptidase IV inhibitors. *Journal of Medicinal Chemistry* 48: 6991–6996.

Weber, A.E. 2004. Dipeptidyl peptidase IV inhibitors for the treatment of diabetes. *Journal of Medicinal Chemistry* 47: 4135–4141.

Xu, J., L. Wei, R.J. Mathvink, S.D. Edmondson, G.J. Eiermann, H. He, J.F. Leone, B. Leiting, K.A. Lyons, F. Marsilio, R.A. Patel, S.B. Patel, A. Petrov, G. Scapin, J.K. Wu, N.A. Thornberry, and A.E. Weber. 2006. Discovery of potent, selective, and orally bioavailable oxadiazole-based dipeptidyl peptidase IV inhibitors. *Bioorganic & Medicinal Chemistry Letters* 16: 5373–5377.